

*Electronic supplementary information for*

## **Robust Single-Mode Lasers Based on Hexagonal CdS Microflakes**

Yang Mi,<sup>\*a</sup> Yaoyao Wu,<sup>a</sup> Jinchun Shi,<sup>\*b</sup> Sheng-Nian Luo<sup>a</sup>

<sup>a</sup>Key Laboratory of Advanced Technologies of Materials, Ministry of Education, and Institute of Material Dynamics, Southwest Jiaotong University, Chengdu, Sichuan 610031, P. R. China.  
Email: miyang@swjtu.edu.cn

<sup>b</sup>The Peac Institute of Multiscale Sciences, Chengdu, Sichuan 610031, P. R. China  
Email: jcshi@pims.ac.cn

## *Contents*

- (1) **Fig. S1** AFM images and corresponding height profiles of two CdS microflakes.
- (2) **Fig. S2** SAED patterns taken from the hexagonal CdS microflake.
- (3) **Fig. S3** Setup for photoluminescence and lasing characterizations with a  $\mu$ -PL system.
- (4) **Fig. S4** The simulated spectrum in the small cavity by numerical simulation.
- (5) **Fig. S5** Enlarged emission spectra of a typical CdS hexagonal microflake at different optical pump fluences.
- (6) **Fig. S6** The relative output power of the center peak longitudinal mode and side-mode peaks of the laser.
- (7) **Fig. S7** Emission spectra of a large CdS hexagonal microflake at different optical pump fluences.
- (8) **Fig. S8** The decay profiles of the emission from a typical CdS microflake at different optical pump fluences.
- (9) **Fig. S9** The decay profiles of the reference sample and hexagonal CdS microflakes with different sizes.
- (10) **Table S1** Fitting parameters for TRPL decay profiles in Fig. 4a using the Gaussian response function convoluted with the di-exponential decays function.
- (11) **Table S2** Fitting parameters for TRPL decay profiles in Fig. 4b using the Gaussian response function convoluted with the di-exponential decays function.

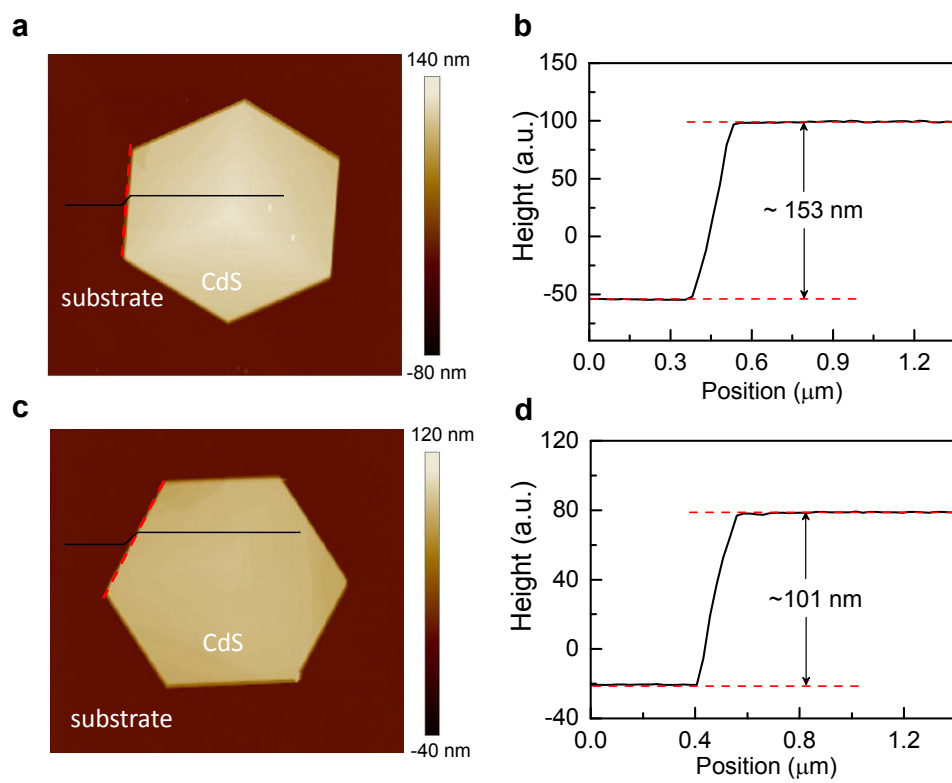


**Fig. S1** AFM images and corresponding height profiles of individual CdS microflakes with different heights of  $\sim 153$  and 101 nm.

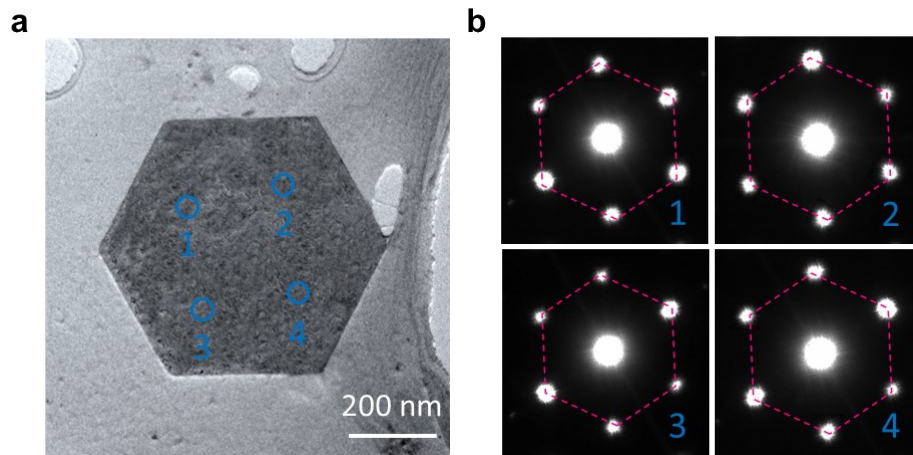


**Fig. S2** SAED patterns taken from the areas labeled with numbers 1-4 (blue) in the hexagonal CdS microflake.

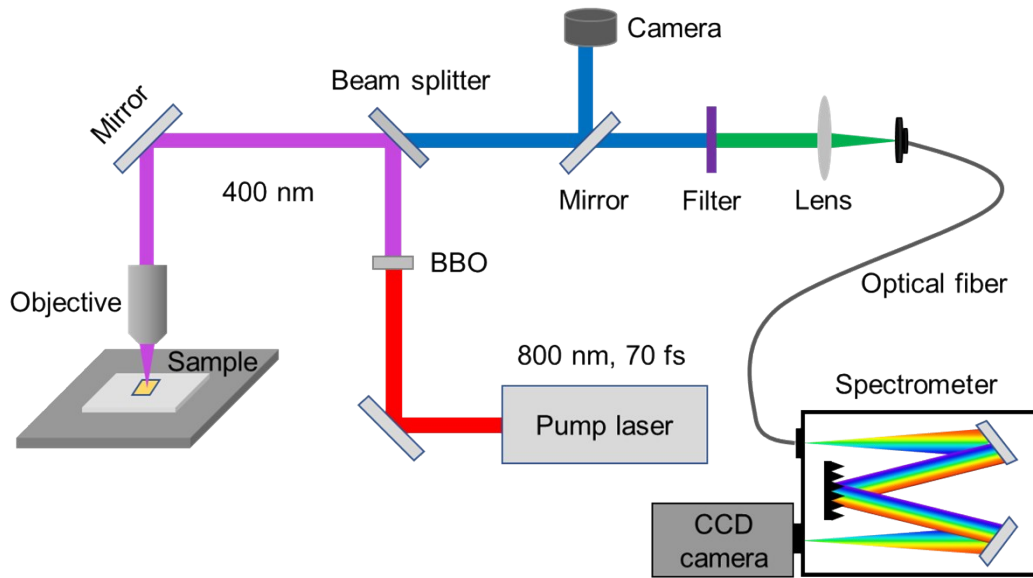


**Fig. S3** Setup for photoluminescence and lasing characterizations with a  $\mu$ -PL system.

The 400 nm pulsed laser was generated by frequency doubling the output (with a BBO crystal) from a Ti:sapphire oscillator (Femtosource XL300, Spectra-Physics; 800 nm, 70 fs, 5 MHz). The pump laser beam was introduced into the optical microscope and focused to  $\sim 4 \mu\text{m}$  in diameter by a microscope objective (RMS20 $\times$ , NA: 0.45, OLYMPUS) to excite the microflakes to minimize heat and optical damage at high energy pump condition and promote energy injure efficiency. The backscattered emission signal was collected by the same objective and analyzed by a spectrometer (IsoPlane SCT320, Princeton Instruments) with a  $1200 \text{ mm}^{-1}$  grating and a TE-cooled charge coupled device camera (BLAZE, Princeton Instruments). A 442 nm long pass filter was placed before the optical fiber to block the pump laser.

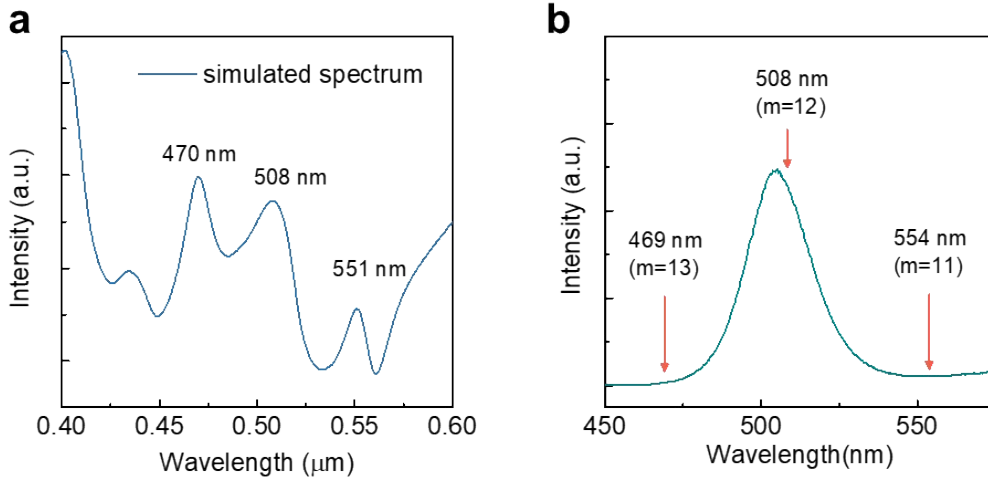


**Fig. S4** (a) The simulated spectrum in the small cavity (side length:  $\sim 850$  nm; thickness:  $\sim 100$  nm) via numerical simulation, showing the theoretical adjacent modes around 470 and 551 nm, respectively. (b) PL spectrum of an individual CdS microflake, the theoretical modes at 554 nm and 469 nm are unavailable within the width of optical gain spectrum.

In principle, a single-mode laser can be achieved in small cavities by extending the mode spacing, until only one oscillation mode survives in the bandwidth of optical gain.<sup>1, 2</sup> For a WGM microcavity, we have the following equation for the fundamental modes:<sup>3, 4</sup>

$$m\lambda_m = (m+1)\lambda_{m+1} = nL$$

where  $n$  is the effective index,  $L$  is the cavity length of the WGM microcavity,  $\lambda_m$  and  $\lambda_{m+1}$  are the resonance wavelengths of two successive modes. Given that  $m=12$  and  $\lambda_m=508.1$  nm in the cavity, the theoretical adjacent modes  $\lambda_{11}$  and  $\lambda_{13}$  are estimated to be around 553 nm ( $m=11$ ) and 469 nm ( $m=13$ ), respectively. The corresponding simulated spectrum in **Fig. S4a** shows the theoretical adjacent peaks around 470 and 551 nm, which are consistent with the predicted modes. However, both of the theoretical modes are unavailable within the width of optical gain spectrum, as shown in **Fig. S4b**. Therefore, we cannot observe a spectrum modulated by a number of peaks with the characteristic WGM distribution in such a microcavity. The characteristic WGM modulated spectra can only be realized in larger sized cavities with high mode order and enough bandwidth.<sup>5</sup> Therefore, the free-spectral range in such small CdS cavity is larger than the width of optical gain spectrum, single-mode lasing can be achieved.

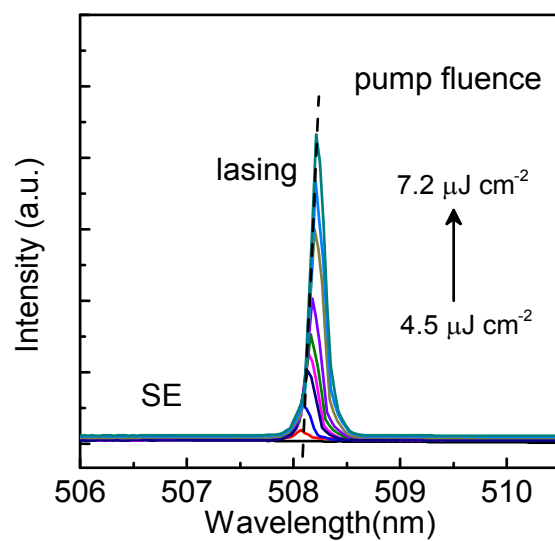


**Fig. S5** Magnified emission spectra of a typical CdS hexagonal microflake at different optical pump fluences from 4.5 to 7.2  $\mu\text{J}/\text{cm}^2$ , which shows the red shift of the lasing peak with increasing pump fluence.

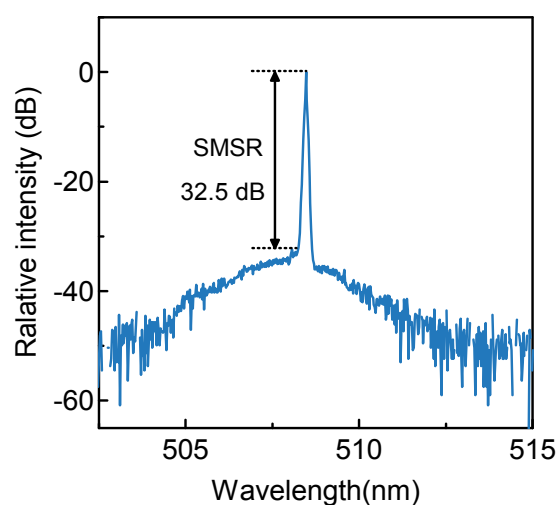


**Fig. S6** The relative output power of the center peak longitudinal mode and side-mode peaks of the laser extracted from Fig. 2b at the pump fluence of  $7.2 \mu\text{J}/\text{cm}^2$ . The laser shows an estimated SMSR of 32.5 dB, indicating most of the power exists in the main mode.

The side-mode suppression ratio (SMSR) of a laser describes the relation of output power between the center peak longitudinal mode and the largest side mode in decibel (dB),<sup>6</sup> which is an important parameter of the longitudinal mode. Limited to the experiment setup (the optical spectrum analyzer is unavailable), the output power at different wavelengths and the SMSR was not measured in the spectra of the laser. From the lasing spectra, the accurate output power at different wavelengths is unavailable. Alternatively, we estimated the mode offset (the relative power) at different wavelength in units of dB using the following equation:  $\text{dB}=10\log I$ , where  $I$  stands for the emission intensity of the PL. **Fig. S6** shows the relative output power of the main peak and side-mode peaks of the laser extracted from Fig. 2b at the pump fluence of  $7.2 \mu\text{J}/\text{cm}^2$ . The laser achieves an estimated SMSR of 32.5 dB, indicating most of the power exists in the main mode.



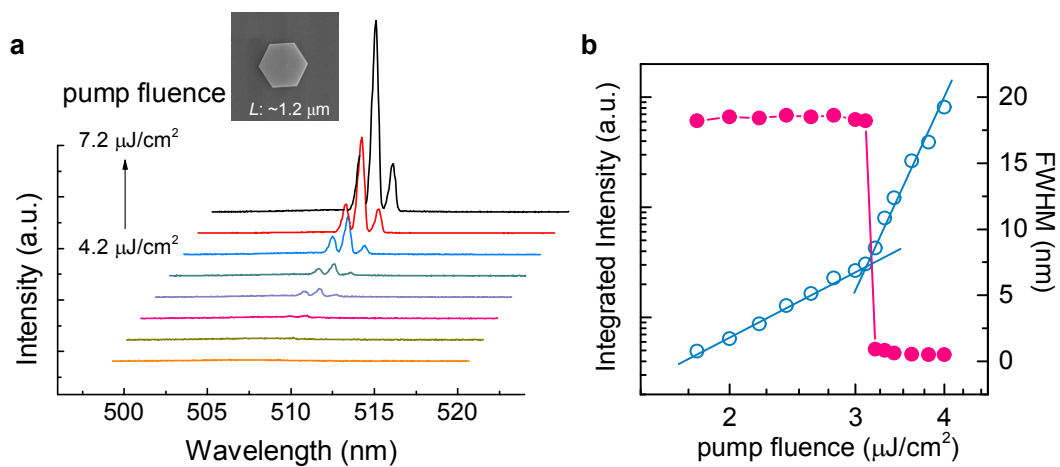


**Fig. S7** (a) Emission spectra of a typical CdS hexagonal microflake ( $L$ :  $\sim 1.2 \mu\text{m}$ ) at different optical pump fluences from 4.2 to  $7.2 \mu\text{J}/\text{cm}^2$ . (b) The integrated PL intensity and FWHM of the microflake as a function of pump fluence.

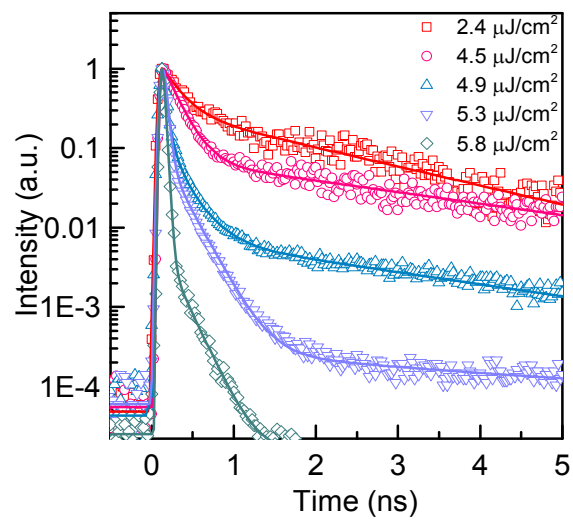


**Fig. S8** The decay profiles of the emission from a typical CdS microflake measured under the pump fluence of 2.4, 4.5, 4.9, 5.3, and 5.8  $\mu\text{J}/\text{cm}^2$ , respectively. Solid lines are the fitted results.

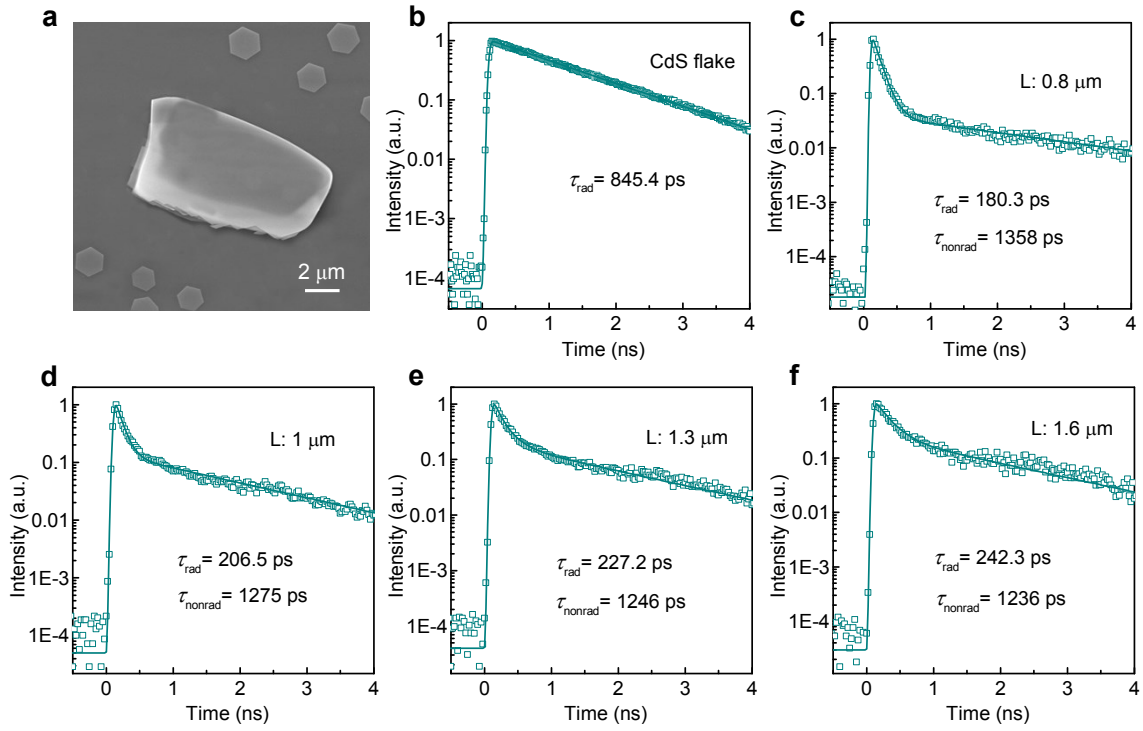


**Fig. S9** (a) SEM image of a large irregular CdS flake on mica substrate. (b-f) The decay profiles of the reference sample (length:  $\sim 9.5 \mu\text{m}$ ; width:  $\sim 4.5 \mu\text{m}$ ) and hexagonal CdS microflakes with different sizes. The side lengths of the platelets in c, d, e and f are  $\sim 0.8$ , 1, 1.3, and 1.6  $\mu\text{m}$ , respectively. Solid lines are the fitted results.

### TRPL Decay profile fitting

A Gaussian response function convoluted with bi-exponential model was used to fit the TRPL decay trace in Fig. 4, the TRPL traces  $I(t)$  can be described by Equation (1) below,

$$I(t)=A_1 \exp (-t/\tau_1) +A_2 \exp (-t/\tau_2) \quad (1)$$

where  $A_1$  and  $\tau_1$  ( $A_2$  and  $\tau_2$ ) represent the fast (slow) decay components, and  $\tau_1 < \tau_2$ .

**Table S1.** Fitting parameters for TRPL decay profiles of a typical CdS microflake at different pump fluences in Fig. 4a using the Gaussian response function convoluted with the bi-exponential decays function.

Pump fluence ( $\mu\text{J}/\text{cm}^2$ )	Decay time (ps)	Amplitude (%)
2.4	$t_1=214.3\pm 6.9$	85.2
	$t_2=1412\pm 43$	14.8
4.1	$t_1=180.3\pm 5.8$	88.9
	$t_2=1658\pm 32$	11.1
4.9	$t_1=46.4\pm 3.4$	94.6
	$t_2=258.3\pm 18.2$	5.4
5.3	$t_1=35.2\pm 2.9$	96.4
	$t_2=222.4\pm 15.3$	3.6
5.8	$t_1=23.4\pm 1.9$	99.9
	$t_2=192.4\pm 12.6$	0.1

**Table S2.** Fitting parameters for TRPL decay profiles of CdS microflakes with different side lengths in Fig. 4b using the Gaussian response function convoluted with the monoexponential and di-exponential decays function.

Side length ( $\mu\text{m}$ )	Decay time (ps)	Amplitude (%)
reference	$t=845.4\pm 9.2$	100
1.6	$t_1=242.3\pm 7.2$	80.6
	$t_2=1236\pm 42$	19.4
1.3	$t_1=227.2\pm 6.9$	82.8
	$t_2=1246\pm 48$	17.2
1	$t_1=206.5\pm 5.7$	84.5
	$t_2=1275\pm 58$	15.5
0.8	$t_1=180.3\pm 5.8$	86.9
	$t_2=1358\pm 32$	13.1

#### References:

1. A. Javan, W. R. Bennett Jr and D. R. Herriott, *Phys. Rev. Lett.*, 1961, **6**, 106-110.
2. J. Zayhowski and A. Mooradian, *Opt. Lett.*, 1989, **14**, 618-620.
3. V. D. Ta, R. Chen, L. Ma, Y. J. Ying, H. D. Sun, *Adv. Mater.*, 2012, **24**: OP60-OP64.
4. S. C. Yang, Y. Wang, H. D. Sun, *Adv. Opt. Mater.*, 2015, **3**, 1136.
5. Grivas C, Li C, Andrekou P, et al. *Nat Commun.*, 2013, **4**: 2376.
6. S. L. Woodward, I. M. I. Habbab, T. L. Koch and U. Koren, *IEEE Photonics Technology Letters*, 1990, **12**, 854-856.